



HAL
open science

The relative contribution of fleshy epiphytic macroalgae to the production of temperate maerl (rhodolith) beds

Zn Qui-Minet, Dominique Davoult, J Grall, Sophie Martin

► **To cite this version:**

Zn Qui-Minet, Dominique Davoult, J Grall, Sophie Martin. The relative contribution of fleshy epiphytic macroalgae to the production of temperate maerl (rhodolith) beds. *Marine Ecology Progress Series*, In press, 693, pp.69-82. 10.3354/meps14089 . hal-03692321

HAL Id: hal-03692321

<https://hal.science/hal-03692321>

Submitted on 9 Jun 2022

HAL is a multi-disciplinary open access archive for the deposit and dissemination of scientific research documents, whether they are published or not. The documents may come from teaching and research institutions in France or abroad, or from public or private research centers.

L'archive ouverte pluridisciplinaire **HAL**, est destinée au dépôt et à la diffusion de documents scientifiques de niveau recherche, publiés ou non, émanant des établissements d'enseignement et de recherche français ou étrangers, des laboratoires publics ou privés.

14 **ABSTRACT**

15

16 Maerl beds are composed of unattached red calcareous coralline algae. When located in
17 shallow ecosystems, these calcareous macroalgae provide substrates for the development of
18 fleshy epiphytic macroalgae, which contribute to the productivity of maerl beds. To assess
19 the importance of their contribution, we estimated the primary production of the main taxa
20 of fleshy epiphytic macroalgae (*Solieria chordalis* or Rhodomelaceae), growing in two
21 distinct *Lithothamnion corallioides* maerl beds of the Bay of Brest (Brittany, France)
22 characterized by different depths and incident irradiances. We estimated epiphytic algal
23 photosynthetic parameters derived from photosynthesis-irradiance curves calculated from
24 incubations in photo-respirometry chambers at different irradiances and in the dark. A
25 comparison with results previously obtained in *L. corallioides* showed that, in the two studied
26 maerl beds, there were no differences between maerl and its fleshy epiphytic macroalgae in
27 terms of photo-acclimation to low irradiances. However, fleshy epiphytic macroalgae had
28 higher photosynthetic efficiencies and photosynthetic rates per unit of biomass or chlorophyll
29 *a* than the maerl species. Estimations of net primary production per surface area of maerl bed
30 indicated that fleshy epiphytic macroalgae account for 25% of maerl bed productivity.
31 Interactions between *L. corallioides* and its fleshy epiphytic macroalgae may affect their
32 respective contributions. In the deepest maerl beds, shading by fleshy epiphytic macroalgae
33 may have a detrimental impact on *L. corallioides* net primary production, whereas in the
34 shallowest maerl beds, fleshy epiphytic macroalgae may protect maerl from photoinhibition
35 under high irradiances.

36 **Keywords:** maerl, fleshy epiphytic macroalgae, photosynthesis, productivity, red algal
37 physiology, *Solieria chordalis*, filamentous Rhodomelaceae

38 1. INTRODUCTION

39 Macroalgae acting as ecosystem engineers form macroalgal beds, which are among the most
40 productive habitats in coastal marine systems (Olafsson 2016). Their contribution to the
41 biogeochemical cycles is tightly linked to the incident irradiance they receive and their
42 metabolic rates (Hurd et al. 2014). Among macroalgal foundation species, free-living red
43 calcareous coralline algae (known as maerl) are long-lived species that grow worldwide at
44 different depths, from the surface under high irradiances down to 250 m under dim-light
45 conditions (Amado-Filho et al. 2017; Riosmena-Rodríguez et al. 2017). Although very slow-
46 growing, maerl algae can accumulate, constituting vast beds of high density and biomass,
47 thus significantly contributing to marine coastal primary production (Martin et al. 2007, van
48 der Heijden & Kamenos 2015).

49 When located in shallow environments, maerl beds are home to a highly diverse flora (Peña
50 et al. 2014). Maerl bed flora have been assessed in tropical ecosystems (Brazil, Amado-Filho
51 et al. 2010), in the Mediterranean (Ustica Island, Mannino et al. 2002) and in the Northeast
52 Atlantic, from Svalbard to Portugal (Peña et al. 2014). These studies have highlighted that
53 maerl algae harbor higher diversity and abundance of red fleshy epiphytes than brown and
54 green epiphytes. In the NE Atlantic, maerl beds are found from the intertidal zone down to
55 60 m depth (Hernández-Kantún et al. 2017). Most beds are patchily distributed and found at
56 less than 30 m depth (Peña et al. 2014), where light conditions are also favorable for the
57 growth of fleshy epiphytic macroalgae. NE Atlantic maerl beds harbor at least 50 fleshy
58 epiphytic macroalgal species, mostly Rhodophyta (Peña et al. 2014). In contrast to maerl
59 species, fleshy epiphytic macroalgae are fast-growing, short-lived organisms. Their
60 composition and biomass depend on environmental factors favorable to their growth, such as
61 high temperature, light, and nutrient availability (Qui-Minet et al. 2018, 2021). Habitat

62 stability and variations in maerl morphology also influence fleshy epiphytic macroalgal
63 abundance and species composition (Pascelli et al. 2013). The hydrodynamic regime,
64 including winter storm disturbances, affects the abundance of fleshy epiphytic macroalgae in
65 maerl beds (Amado-Filho et al. 2010, Qui-Minet et al. 2018). It also determines maerl
66 morphology and, in turn, influences its associated macroflora (Bosence 1976).

67 The contribution of fleshy epiphytic macroalgae to the primary production of maerl beds thus
68 depends on various environmental factors. It also depends on the living biomass of epiphytic
69 macroalgal taxa and on their capacity to capitalize on the incident irradiance they receive. In
70 the Bay of Brest (Brittany, France), the seasonality of maerl bed flora likely plays a major
71 role in community primary production (Martin et al. 2007). Epiphytic macroalgal species
72 distribution and abundance vary with season (Grall 2002) and local environmental changes
73 (Grall 2002, Qui-Minet et al. 2018). Their contribution to carbon budgets in temperate
74 ecosystems can be particularly important in summer due to their higher abundance during
75 this season (Grall 2002, Guillou et al. 2002, Qui-Minet et al. 2018).

76 The contribution of epiphytic red macroalgae to maerl bed productivity also depends on
77 specific photo-physiological performance of epiphyte species (Hurd et al. 2014). Although
78 the physiology of maerl algae has been well studied (Martin et al. 2006, Schoenrock et al.
79 2018, Qui-Minet et al. 2019, Sordo et al. 2020, Qui-Minet et al. 2021), no study has assessed
80 the physiology of red fleshy macroalgae inhabiting maerl beds. Maerl algae are known to
81 show a high capacity for acclimation or adaptation to different depths/irradiances. For
82 instance, in the Bay of Brest (Brittany, France), where *Lithothamnion corallioides* is the
83 dominant maerl alga, summer irradiances of saturation in this species range from 100 to 200
84 $\mu\text{mol photon m}^{-2} \text{ s}^{-1}$, depending on its location (depth and light availability) and thallus

85 morphology (Martin et al. 2006, Qui-Minet et al. 2021). Maximal gross production rates in
86 *L. corallioides* are observed in summer, ranging from 1 to 3 $\mu\text{mol O}_2 \text{ g}^{-1} \text{ DW h}^{-1}$.

87 Some studies have assessed the physiology of red fleshy macroalgae, including Rhodophyta
88 genera known to grow in temperate maerl beds of the NE Atlantic (Dudgeon et al. 1995,
89 Johansson & Snoejis 2002, Michler et al. 2002, McCoy et al. 2019). A study on several
90 species of red macroalgae from the Baltic Sea and the Skagerrak (Gullmar Fjord) highlighted
91 a high species-dependent variability in maximal gross production rates, ranging from 70 to
92 500 $\mu\text{mol O}_2 \text{ g}^{-1} \text{ DW h}^{-1}$ in summer (Johansson & Snoejis 2002). The saturating irradiances
93 in these species are strongly related to water depth (and irradiances), with values ranging
94 from 100 to 300 $\mu\text{mol photons m}^{-2} \text{ s}^{-1}$ for species typical of the upper littoral (0–5 m depth)
95 and lower values (i.e. $<100 \mu\text{mol photons m}^{-2} \text{ s}^{-1}$) for species typical of the lower littoral
96 (below 10 m depth).

97 The contribution of epiphytic algae to the productivity of vegetated marine coastal
98 ecosystems has been mainly studied in seagrass beds (Moncreiff & Sullivan 2001,
99 Borowitzka et al. 2006), but remains relatively poorly understood in macroalgal habitats
100 despite the potentially high biomass of fast-growing epiphytes that may contribute
101 significantly to the total productivity of these ecosystems. The epiphytic algae of seagrasses
102 are important primary producers that can indeed make up a significant proportion (up to 60%)
103 of the total primary production of seagrass beds (Borowitzka et al. 2006, Berlinghof et al.
104 2022). In contrast, epiphytic macroalgae of the kelp species *Laminaria hyperborea* contribute
105 little to the total productivity of the entire kelp forest, relative to the kelp itself (Pedersen et
106 al. 2014). The contribution of fleshy epiphytic macroalgae to the primary production of maerl
107 beds has never been assessed. The lack of knowledge on the physiology of fleshy epiphytic

108 macroalgae limits our ability to evaluate their contribution to the productivity of macroalgal
109 ecosystems.

110 The main objective of this work was to estimate the relative contribution of fleshy epiphytic
111 macroalgae to the maerl bed productivity as a function of bottom incident irradiance
112 variability. For the first time, we determined photosynthetic parameters of temperate fleshy
113 macroalgal maerl epiphytes and we estimated their rates of primary production and their
114 contribution to carbon budgets in two distinct maerl beds of the Bay of Brest (two stations),
115 characterized by different depths/incident irradiances, macroalgal biomasses and epiphytic
116 taxa. Macroalgae physiological parameters were measured in summer, when fleshy epiphytic
117 macroalgal biomass reaches its highest peak in the Bay of Brest (Grall 2002, Guillou et al.
118 2002, Peña et al. 2010). Macroalgal productivity per surface unit of maerl bed was estimated
119 using previous data on *L. corallioides* and fleshy epiphytic macroalgal biomass and *L.*
120 *corallioides* physiology (Qui-Minet et al. 2018, 2021). Our working hypotheses were i)
121 physiological characteristics differ between epiphytic macroalgae according to taxon and
122 specific environmental conditions at the two stations, and ii) fleshy epiphytic macroalgae
123 have higher production rates than maerl (*L. corallioides*), and thereby significantly contribute
124 to the productivity of maerl beds in summer.

125

126 **2. MATERIALS AND METHODS**

127

128 *2.1 Study site*

129 Epiphyte and maerl primary production rates were studied at two stations (A and B) in the
130 Bay of Brest (Britany, France), where maerl beds cover almost one third of its bottom surface.

131 Mean tidal range in the bay is 4 m, and minimal and maximal tidal ranges are 0.3 and 8 m,
132 respectively. Station A is located in the northern basin of the bay (48°21'57"N, 04°26'47"W),
133 and Station B is located in the southern basin (48°19'58"N, 04°19'57"W). Chart datum is
134 2.5 m at Station A and 0.7 m at Station B.

135 In the Bay of Brest, bottom currents have a significant impact on macroalgal assemblages
136 (Qui-Minet et al. 2018). Summer fleshy epiphytic macroalgal biomass (DW) ranges from 21
137 to 49 g m⁻² at Station A and from 13 to 23 g m⁻² at Station B, with no significant statistical
138 differences between them (Qui-Minet et al. 2018). Filamentous Rhodomelaceae are dominant
139 at Station A. Peña et al. (2014) identified the five filamentous Rhodomelaceae species present
140 in Brittany (France): *Polysiphonia elongata*, *P. fibrillosa*, *P. fucoides*, *P. fucellata*, *P. nigra*,
141 *P. stricta* and *P. subulifera*. A recent revision of the *Polysiphonia* genus (Díaz-Tapia et al.
142 2017) has split this group of fleshy epiphytic macroalgal species into four genera:
143 *Polysiphonia*, *Carrodoriella*, *Leptosiphonia* and *Verebrata*. Identification to the species level
144 at Station A was not possible in the present study; we thus refer this taxon as “filamentous
145 Rhodomelaceae”, the main fleshy epiphytic macroalgae at this location. At Station B, the
146 dominant species was *Solieria chordalis*. Filamentous Rhodomelaceae and *S. chordalis* differ
147 in their morphology. Filamentous Rhodomelaceae include taxa with multiaxial morphology
148 in which upright filaments are laterally or dichotomously branched (polysiphonous
149 morphology), whereas *S. chordalis* grows erect from a fibrous basal system and generally
150 has two or three orders of branching (Gabrielson & Hommersand 1982). The living biomass
151 of *Lithothamnion corallioides* is highly variable in maerl beds of the bay, but is not
152 significantly different between Station A (from 850 to 8550 g m⁻²) and Station B (from 3100
153 to 5650 g m⁻²) (Qui-Minet et al. 2018).

154 2.2 Incubation procedure and physiological measurements

155 In the Bay of Brest, September is representative of the summer period in terms of temperature
156 and irradiance (Martin et al. 2007, Qui-Minet et al. 2021). Maximal metabolic rates are
157 reached during this period in maerl beds of the Bay of Brest (Martin et al. 2007).
158 Physiological measurements were carried out on 17 September 2015 under the following
159 physico-chemical conditions: temperature, $17.8 \pm 0.2^{\circ}\text{C}$ [Station A] and $16.3 \pm 0.0^{\circ}\text{C}$
160 [Station B]; salinity, 35.1 ± 0.0 [A] and 35.0 ± 0.0 [B], and pH 7.92 ± 0.03 [A] and $8.03 \pm$
161 0.02 [B]. *L. corallioides* physiological measurements were taken on 16–18 September 2015
162 (see Qui-Minet et al. (2021) under similar physico-chemical conditions and using the same
163 methodology as that described below for epiphytes.

164 Algae were collected with a Van Veen grab (5 replicates of 0.1 m^2 per station), rinsed with
165 filtered seawater on a 5 mm mesh sieve and then carefully cleaned to remove the sediments.
166 The most abundant fleshy epiphytic taxa of each station were identified and selected as
167 filamentous Rhodomelaceae (Station A) or *Solieria chordalis* (Station B), both taxa being
168 free of epiphytes.

169 Measurements were carried out by incubating the most abundant fleshy epiphytic algal taxon
170 at each station. Macroalgal incubations were performed in the light and in the dark. During
171 incubations, surface irradiance in terms of photosynthetically active radiation (PAR, μmol
172 $\text{photons m}^{-2} \text{ s}^{-1}$) was recorded every minute using a LI-COR quantum sensor (LI 192 SA).
173 Maximum surface irradiance ranged from to 570 to 1100 $\mu\text{mol photons m}^{-2} \text{ s}^{-1}$. Macroalgal
174 net photosynthesis (NPP) was measured under different irradiances: maximum surface
175 irradiance (100%), and reduced irradiance levels (65%, 47%, 27%, 13% and 6%), using clear
176 chambers and opacifying neutral filters. Respiration (R) was measured in the dark using dark
177 chambers. NPP and R rates were obtained by measuring the initial and final oxygen
178 concentration with an oxygen probe (Oxymeter HQ40D, Hatch Lange, Ltd. portable LDOTM)

179 at the beginning and at the end of the incubations. For each level of irradiance and in the
180 dark, five photo-respirometry chambers (220 mL) were filled with bottom seawater and
181 fleshy epiphytic macroalgae (algal dry mass of 0.5-1 g DW). Five photo-respirometry
182 chambers were only filled with bottom seawater and used as controls. Bottom seawater was
183 collected at each station (approximately 1 m above the bottom) in a Niskin bottle. Incubations
184 were performed on board the R/V *Albert Lucas* immediately after collecting the algae.
185 Chambers were kept in a water bath with a continuous flow of water coming from the bottom
186 at the *in situ* temperature. Incubations lasted 1 hour to avoid oxygen saturation greater than
187 120% during light incubations and to maintain oxygen saturation above 80% at the end of
188 dark incubations.

189

190 2.3 Sample treatment and processing

191 At the end of incubations, algal samples were collected and dried (60°C, 48 h). In parallel,
192 additional samples were rinsed with filtered autoclaved seawater to remove salts, placed in 2
193 mL cryotubes and frozen in liquid nitrogen. Samples were maintained at -80°C prior to
194 lyophilization for pigment analyses. To obtain a fine powder, samples were ground in a
195 Tissue Lyser II (QIAGEN) bead mill in plastic tubes using 0.5 cm stainless steel beads
196 (Brammer). Chlorophyll *a* of fleshy epiphytic macroalgae was analyzed using a calibrated
197 Turner 10-AU fluorimeter, according to the Arar & Collins (1997) equation:

198

$$199 \quad C_{S.c.} = \frac{C_{F.c.} \times \text{extract volume (L)} \times DF}{\text{Sample volume (L)}} \quad (1)$$

200 where, $C_{S,c}$ is the corrected chlorophyll *a* concentration ($\mu\text{g/L}$) in the whole water sample,
201 $C_{E.C.}$ is the uncorrected chlorophyll *a* concentration in the water sample ($\mu\text{g/L}$), DF is the
202 dilution factor, and extract volume is the volume (L) of extract prepared before dilution.

203

204 *2.4 Data processing*

205 To obtain actual macroalgal physiological parameters, fluxes were corrected with respect to
206 control data. NPP and R rates were calculated as a function of algal dry weight ($\mu\text{mol O}_2 \text{g}^{-1}$
207 DW h^{-1}) or as a function of algal chlorophyll *a* content ($\mu\text{mol O}_2 \text{mg}^{-1} \text{Chl } a \text{ h}^{-1}$) according
208 to the following equation:

$$209 \quad \text{NPP or R} = \frac{\Delta\text{O}_2 \times V}{\text{Alg} \times \Delta t} \quad (2)$$

210 where ΔO_2 ($\mu\text{mol L}^{-1}$) is the variation of dissolved oxygen concentration between the
211 beginning and the end of the incubation, V (L) is the volume occupied by the seawater in the
212 chamber, Alg is the dry weight (g) or Chl *a* content (mg) of algae in the chamber, Δt (h) is
213 the incubation time. The relationships between irradiance (E , $\mu\text{mol photons m}^{-2} \text{s}^{-1}$) and NPP
214 as a function of algal dry weight or as a function of algal Chl *a* content at a given irradiance,
215 were obtained using the Chalker (1981) equation:

216

$$217 \quad \text{NPP} = \text{GPP}_{\text{MAX}} \times \left(1 - e^{\frac{-E}{Ek}}\right) - R \quad (3)$$

218 Where GPP_{MAX} is the maximal gross primary production expressed in terms of algal dry
219 weight (in $\mu\text{mol O}_2 \text{g}^{-1} \text{DW h}^{-1}$) or algal Chl *a* content ($\mu\text{mol O}_2 \text{mg}^{-1} \text{Chl } a \text{ h}^{-1}$). Ek (μmol
220 $\text{photons m}^{-2} \text{s}^{-1}$) is the saturating irradiance for photosynthesis and R is the respiration rate
221 (in $\mu\text{mol O}_2 \text{g}^{-1} \text{DW h}^{-1}$ or $\mu\text{mol O}_2 \text{mg}^{-1} \text{Chl } a \text{ h}^{-1}$).

222 The compensation irradiance (E_c , $\mu\text{mol photons m}^{-2} \text{s}^{-1}$) is the irradiance at which NPP = 0
223 (or GPP = R). Alpha (α), the photosynthetic efficiency ($\mu\text{mol O}_2 \text{ g}^{-1} \text{ h}^{-1} (\mu\text{mol photons m}^{-2} \text{ s}^{-1})^{-1}$)
224 was calculated using the following equations:

$$225 \quad \alpha = \frac{GPP_{MAX}}{Ek} \quad (4)$$

226 At each station, values of bottom irradiance were calculated using chart datum, tidal height
227 and light extinction coefficients measured at each station during the summer season (0.38 for
228 Station A and 0.43 for Station B). Bottom incident irradiance was calculated every 20 min
229 from surface irradiance data (SOMLIT-MAREL), tidal ranges (www.maree.info) and light
230 extinction coefficients previously obtained for summer season at each station (Qui-Minet et
231 al. 2018). Surface irradiance (PAR) was monitored at high frequency (every 20 min) by the
232 autonomous COAST-HF-MAREL-Iroise buoy (MAREL-Iroise/SOMLIT-Brest scientific
233 platform) located in the Bay of Brest. Summer is here defined as the period from 16 June to
234 15 September 2015. Values of NPP (mg C m^{-2}) per h (or per day) were individually estimated
235 for *L. corallioides*, filamentous Rhodomelaceae and *S. chordalis* using photosynthesis-
236 irradiance (P-E) parameters presented here (epiphytes) or previously published (maerl, Qui-
237 Minet et al. 2021), algal biomass data per m^2 (Qui-Minet et al. 2018) and calculated bottom
238 irradiance values. Data were obtained in terms of $\mu\text{mol O}_2 \text{ m}^{-2} \text{ h}^{-1}$ or $\mu\text{mol O}_2 \text{ m}^{-2} \text{ day}^{-1}$ and
239 converted from μmol of O_2 to mg C , using photosynthetic and respiration quotients (PQ and
240 RQ, respectively) previously reported for *L. corallioides* (PQ:1.17 and RQ:0.97, Martin et
241 al. 2006) and for red fleshy macroalgae (PQ:1.20, Buesa 1980; RQ:1.00, Carvalho & Eyre
242 2011), and the molecular weight of C. In addition to the estimations of macroalgal NPP (mg
243 $\text{C m}^{-2} \text{ day}^{-1}$), we give the 24 h NPP rates ($\text{mg C m}^{-2} \text{ h}^{-1}$) during three specific days with

244 contrasting tidal ranges: low water neap tide (LWNT, “low” tidal range of 1–2 m), medium
245 water tide (MWT, “medium” tidal range of 4 m) and high water spring tide (HWST, “high”
246 tidal range of 6–8 m).

247

248 *2.5 Statistical treatment*

249 Statistical analyses were done using *R Statistical Software* (version 4.1.1). The significance
250 of the fitted curves was tested using the Fisher test. Because data did not follow a normal
251 distribution (Shapiro-Wilk test) and/or the homogeneity of variances (Bartlett test), a non-
252 parametric test (Kruskal-Wallis test) was used to compare fleshy epiphytic macroalgae P-E
253 parameters between stations, bottom irradiance between stations (during the early morning,
254 late morning, afternoon and evening) and NPP rates between taxa/stations. When necessary,
255 tests were followed by a post-hoc Wilcoxon test (pairwise Wilcoxon-test, Wp).

256

257 **3. RESULTS**

258 *3.1 Comparison of photosynthesis characteristics between filamentous Rhodomelaceae and* 259 *Solieria chordalis*

260 Mean rates of respiration (R) and of maximal gross primary production (GPP_{MAX}) rates were
261 significantly higher in filamentous Rhodomelaceae than in *S. chordalis* (Fig. 1 & Table 1).
262 In contrast, when physiological rates were normalized to the algal chlorophyll *a* (Chl *a*)
263 content, GPP_{MAX} was significantly lower in filamentous Rhodomelaceae than in *S. chordalis*
264 (Fig. 2 & Table 1). Irradiance of saturation (E_k) and irradiance of compensation (E_c) were
265 significantly higher in filamentous Rhodomelaceae than in *S. chordalis* (Table 1).

266

267 3.2. Comparison of photosynthesis characteristics between fleshy epiphytic macroalgae and
268 maerl within and between stations

269 The physiological rates expressed in terms of algal Chl *a* content for *Lithothamnion*
270 *corallioides* and its fleshy epiphytic macroalgae were compared within stations A and B. At
271 Station A, GPP_{MAX} in *L. corallioides* was five times lower than in filamentous
272 Rhodomelaceae. At Station B, it was 12-fold lower than in *S. chordalis* (Table 2 & Fig. 2a-
273 b). *L. corallioides* photosynthetic efficiency (α) coefficients were 6-fold and 12-fold lower
274 than those of fleshy epiphytic macroalgae at stations A and B, respectively (Table 2 & Fig.
275 2a-b). *L. corallioides* R was 3-fold and 11-fold lower than that of fleshy epiphytic macroalgae
276 at stations A and B, respectively (Table 2 & Fig. 2a-b). Within each station, no significant
277 differences in terms of E_k and E_c were observed between *L. corallioides* and its fleshy
278 epiphytic macroalgae.

279

280 3.3 Comparison of diel cycles in incident irradiance

281 Mean bottom irradiance during the summer season was significantly different between the
282 two stations (Fig. 3). Bottom irradiance was significantly lower at Station A than at Station
283 B during the early morning (6–9:00 h), the late morning (9–12:00 h), the afternoon (12–17:00
284 h) and the evening (17–22:00 h) (Table 3). Median values of bottom irradiance during the
285 early morning were 5 and 10 $\mu\text{mol photons m}^{-2} \text{s}^{-1}$ at stations A and B, respectively. They
286 were below the E_c values for *L. corallioides* (16 and 13 $\mu\text{mol photons m}^{-2} \text{s}^{-1}$ at stations A
287 and B, respectively), filamentous Rhodomelaceae (19 $\mu\text{mol photons m}^{-2} \text{s}^{-1}$, Station A) and
288 *S. chordalis* (13 $\mu\text{mol photons m}^{-2} \text{s}^{-1}$, Station B). During the late morning, median values of
289 bottom irradiance remained above E_c and below E_k for the macroalgae taxa here studied.

290 During the afternoon, median values of bottom irradiance were below E_k for *L. corallioides*
291 and filamentous Rhodomelaceae at Station A, whereas at station B median values of bottom
292 irradiance were equal to E_k for *L. corallioides* ($106 \mu\text{mol photons m}^{-2} \text{s}^{-1}$) at Station B. During
293 the evening, median values of bottom irradiance at Station A ($11 \mu\text{mol photons m}^{-2} \text{s}^{-1}$) were
294 below E_c for *L. corallioides* and filamentous Rhodomelaceae, but this was not the case at
295 Station B, where median values of bottom irradiance ($18 \mu\text{mol photons m}^{-2} \text{s}^{-1}$) remained
296 above E_c for *L. corallioides* and *S. chordalis*. In addition to the variability of bottom
297 irradiance among stations, due to surface irradiance and height of tide variability, bottom
298 irradiance also varied significantly among days (Table 3; Fig. 3; Suppl. Figs. 1 & 2).

299

300 3.4. Contribution of fleshy epiphytic macroalgae to NPP at each station

301 Mean rates of net primary production (NPP), estimated from summer average bottom
302 irradiances) at noon were $42 \text{ mg C m}^{-2} \text{ h}^{-1}$ in *L. corallioides* and $10 \text{ mg C m}^{-2} \text{ h}^{-1}$ in
303 filamentous Rhodomelaceae at Station A, and $55 \text{ mg C m}^{-2} \text{ h}^{-1}$ in *L. corallioides* and 16 mg
304 $\text{C m}^{-2} \text{ h}^{-1}$ in *S. chordalis* at Station B (Fig. 5). Comparison of *L. corallioides* and its fleshy
305 epiphytic macroalgae NPP ($\text{mg C m}^{-2} \text{ h}^{-1}$) at both stations during the early morning, late
306 morning, afternoon and evening, showed that NPP $\text{m}^{-2} \text{ h}^{-1}$ varied significantly with tidal
307 rhythms (LWNT, MWT and HWST), being higher in *L. coralloides* than in its fleshy
308 epiphytic macroalgae and at Station B than at Station A. (Table 4; Figs. 4 & 5).

309 Throughout the summer period, diel (24 h) NPP rates ranged from -78 to $178 \text{ mg C m}^{-2} \text{ day}^{-1}$
310 1 in filamentous Rhodomelaceae (Station A) and from -5 to $256 \text{ mg C m}^{-2} \text{ day}^{-1}$ in *S. chordalis*
311 (Station B) (Fig. 7), being significantly higher in *S. chordalis* (KW, $H = 16.2$, $p\text{-value} < 0.001$)
312 (Fig. 7). Diel NPP in *L. corallioides* ranged from -214 to $728 \text{ mg C m}^{-2} \text{ day}^{-1}$ at Station A
313 and from 17 to $808 \text{ mg C m}^{-2} \text{ day}^{-1}$ at Station B, being significantly higher at Station B than

314 at Station A (KW, H = 5.5, p-value <0.05). Diel NPP was significantly higher in *L.*
315 *corallioides* than in fleshy epiphytic macroalgae at both stations (KW, H = 25.3, p-value
316 <0.001 and H = 79.8, p-value <0.001). Diel respiration rates were 145 and 101 mg C m⁻² day⁻¹
317 in filamentous Rhodomelaceae (Station A) and *S. chordalis* (Station B), respectively, being
318 significantly higher in filamentous Rhodomelaceae (KW, H = 154, p-value <0.001). In
319 comparison, diel respiration rates in *L. corallioides* were 470 and of 335 mg C m⁻² day⁻¹ at
320 Stations A and B, respectively, being significantly higher at Station A (KW, H = 154, p-value
321 <0.001). Diel respiration was significantly higher in *L. corallioides* than in fleshy epiphytic
322 macroalgae at both stations (KW, H = 160.0, p-value <0.001). Diel GPP rates ranged from
323 67 to 323 mg C m⁻² day⁻¹ in filamentous Rhodomelaceae (Station A) and from 96 to 357 mg
324 C m⁻² day⁻¹ in *S. chordalis* (Station B), being significantly higher in *S. chordalis* (KW, H =
325 16.2, p-value <0.001) (Fig. 6). Diel GPP in *L. corallioides* ranged from 203 to 1198 mg C m⁻²
326 day⁻¹ at Station A, and from 352 to 1134 mg C m⁻² day⁻¹ at Station B, being significantly
327 higher at Station B (KW, H = 5.5, p-value <0.05) (Fig. 6). Diel GPP was significantly higher
328 in *L. corallioides* than in fleshy epiphytic macroalgae at both stations (KW, H = 130.0, p-
329 value <0.001) (Fig. 6).

330

331 4. DISCUSSION

332 4.1 Epiphytic macroalgal physiology

333 Filamentous Rhodomelaceae and *Solieria chordalis* are ubiquitous, cosmopolitan and
334 opportunistic taxa inhabiting cool temperate shallow coastal areas (Bunker et al. 2017).
335 Filamentous Rhodomelaceae are common in brackish estuaries, in both intertidal and subtidal
336 areas (Baweja et al. 2016). *S. chordalis* generally grows in wave-sheltered habitats, from
337 Ireland to the south of Morocco and the Canary Islands (Guiry & Guiry 2020). Despite

338 knowledge on the ecology of these epiphytic macroalgae, few studies have been carried out
339 on their photosynthesis capacities and their contribution to the primary production or to the
340 C cycle in the coastal ecosystems where they are present remains unknown. Physiological
341 characteristics of algae depend on their local environment. In the Bay of Brest, although light
342 intensity varies considerably at stations A and B, incident bottom irradiance is significantly
343 lower at Station A (deeper) than at Station B (shallower) (Qui-Minet et al. 2018). This
344 difference in environmental conditions suggests that species may show potential photo-
345 acclimation/adaptation to their local environment. The characteristics of photosynthetic
346 parameters of filamentous Rhodomelaceae and *S. chordalis* are typical of shade-growing
347 macroalgae and in agreement with the low incident irradiance they receive at both Station A
348 ($<100 \mu\text{mol photons m}^{-2} \text{ s}^{-1}$) and Station B ($<150 \mu\text{mol photons m}^{-2} \text{ s}^{-1}$) during most of the
349 day due to the turbidity in the Bay of Brest (light extinction coefficients of 0.4 at both stations,
350 Qui-Minet et al. 2018). Accordingly, both taxa displayed low values of compensation
351 irradiance (E_c) and saturation irradiance (E_k) and high photosynthetic efficiency (α), as
352 previously observed in other red macroalgae acclimated to low irradiances (Dawes et al.
353 1999, Johansson G & Snoeijs P 2002). However, despite the distinct depths/incident
354 irradiances at the two stations, lower values of E_c and E_k , and higher values of α and maximal
355 gross primary production (GPP_{MAX}) were observed at the shallower location (Station B) in
356 *S. chordalis* than at the deeper location (Station A) in filamentous Rhodomelaceae,
357 suggesting greater photo-acclimation to low irradiances in *S. chordalis* than in filamentous
358 Rhodomelaceae. This difference in performance is in agreement with the very shallow
359 locations where filamentous Rhodomelaceae are found (Baweja et al. 2016), suggesting that
360 this taxon is better adapted/acclimated to higher irradiances. To survive under a constantly
361 changing light environment and to optimize photosynthesis activity, red macroalgae have

362 evolved several long- and short-term adaptation strategies, such as thallus anatomical
363 changes at the individual level, morphological or organizational changes at the cellular level
364 (long-term adaptation), or functional changes at the molecular level (short-term adaptation)
365 (Talarico & Maranzana 2000).

366 No significant differences were observed between stations in terms of seawater temperature,
367 salinity, pH, or nutrients during the incubations. Nevertheless, due to its shallowness and
368 proximity to freshwater run-off, Station B is characterized by higher variability in physico-
369 chemical parameters (particularly in temperature, salinity, nutrients, and carbonate system
370 parameters) than Station A (Qui-Minet et al. 2018). Hence, differences in physiological
371 parameters, E_c and E_k , between filamentous Rhodomelaceae and *S. chordalis* may be a result
372 of long-term adaptation or short-term acclimation to the station-specific environmental
373 conditions (Talarico & Maranzana 2000) and/or interspecific physiological differences.

374 Morphological differences between epiphytic species are also likely to affect their
375 physiology. Differences in macroalgal morphology translate into differences in the surface
376 area available for dissolved inorganic carbon and nutrient uptake, which result in differences
377 in photosynthetic rates (Wallentinus 1984, Dudgeon et al. 1995, Hurd et al. 1996, Johansson
378 & Snoejis 2002, Roleda & Hurd 2019). Consequently, the polysiphonous structure of
379 filamentous Rhodomelaceae taxa provides them with a higher surface-to-volume ratio and
380 thus higher photosynthesis capacities. Similarly, when comparing photosynthesis capacities
381 of several species from Rhodophyta, Johansson & Snoejis (2002) also observed that species
382 previously classified as *Polysiphonia* spp. (filamentous Rhodomelaceae) are among those
383 with the highest photosynthetic performances: *Polysiphonia brodiaea* (m. *Leptosiphonia*

384 *brodiei*) and *Polysiphonia fucoides* (m. *Vertebrata fucoides*) (350 and 460 $\mu\text{mol O}_2 \text{g}^{-1} \text{h}^{-1}$,
385 respectively).

386

387 4.2 Epiphytic macroalgal physiology vs. maerl physiology

388 Red macroalgal taxa dominate the fleshy epiphytic macroalgal flora in the maerl beds of the
389 Bay of Brest (Qui-Minet et al. 2018) and in other temperate maerl ecosystems (Peña et al.
390 2014). Red algae possess several physiological mechanisms to acclimate to different light
391 intensities (Talarico & Maranzana 2000). In this study, fleshy epiphytic macroalgae also
392 demonstrated a capacity to adapt to deeper and low irradiance environments, with low values
393 of E_c (22 and 15 $\mu\text{mol photons m}^{-2} \text{s}^{-1}$ at stations A and B, respectively) and E_k (171 and 106
394 $\mu\text{mol photons m}^{-2} \text{s}^{-1}$, at stations A and B, respectively). However, due to its calcareous
395 structure, *Lithothamnion corallioides* has lower metabolic rates (per g) than its fleshy
396 epiphytic macroalgae counterparts (GPP rates more than 50-fold higher). Even when
397 photosynthetic rates were normalized to algal Chl *a* content, epiphytic macroalgae had higher
398 rates of GPP and photosynthetic efficiency than *L. corallioides*. Due to their opportunistic
399 nature, these epiphytic species perform better in shaded environments (Burnham et al. 2022).
400 In this respect, the higher surface-to-volume ratio of the thin and filamentous thalli of
401 epiphytic algae maximizes light harvesting (Hurd 2000).

402 Due to their seasonal and patchy presence, fleshy epiphytic macroalgae contribute to the
403 temporal and spatial heterogeneity of the physico-chemical environment by increasing the
404 seawater diel variations in pH, $p\text{O}_2$ and $p\text{CO}_2$ (Semese et al. 2009, Cornwell et al. 2013, Short
405 et al. 2015, Guy-Haim et al. 2020). According to our estimations for the summer season,
406 during sunny days when low tide occurs at noon, bottom irradiances can reach 300 μmol

407 photons $\text{m}^{-2} \text{s}^{-1}$ at Station A and $>500 \mu\text{mol photons m}^{-2} \text{s}^{-1}$ at Station B. Nevertheless, despite
408 its shallowness, the Bay of Brest experiences high turbidity (Qui-Minet et al. 2018) and
409 during the summer season high irradiances are not reached on a daily basis. According to our
410 estimations, maerl beds experience dim irradiances during the early morning and the evening,
411 as well as during rainy/cloudy days. Consequently, fleshy epiphytic macroalgae may
412 overshadow *L. corallioides*, thereby significantly reducing its NPP. According to our
413 estimations, this effect may be detrimental for *L. corallioides* physiology in the early morning
414 and in the evening. In this context, the overall impact of fleshy epiphytic macroalgae on *L.*
415 *corallioides* physiology and survival varies among stations is a function of the patchy
416 distribution of fleshy epiphytic macroalgae, bottom irradiance and macroalgal physiological
417 parameters. Large areas of maerl beds are not covered by fleshy epiphytic macroalgae and,
418 when present, the impact of fleshy epiphytic macroalgae on the incident irradiance received
419 by maerl algae depends on their morphology, density and biomass. Furthermore, under dim
420 irradiances, *L. corallioides* and fleshy epiphytic macroalgae have similar values of E_c (22
421 and $19 \mu\text{mol photons m}^{-2} \text{s}^{-1}$ at Station A, and 15 and $12 \mu\text{mol photons m}^{-2} \text{s}^{-1}$ at Station B,
422 respectively), and compete for light. In our study, incident irradiance differed significantly
423 between stations A and B. At Station A, incident irradiance remained lower than E_k values
424 measured in *L. corallioides* ($171 \mu\text{mol photons m}^{-2} \text{s}^{-1}$, Qui-Minet et al. 2021) and
425 filamentous Rhodomelaceae ($185 \mu\text{mol photons m}^{-2} \text{s}^{-1}$), because during most part of the day,
426 the highest irradiance value remained lower than E_k , reaching $100 \mu\text{mol photons m}^{-2} \text{s}^{-1}$.
427 Therefore, if fleshy epiphytic macroalgae overshadow *L. corallioides*, they may have a
428 negative impact on maerl primary production and subsequently its growth and survival. At
429 Station B, macroalgae experience irradiances higher than E_k (> 150 and up to $600 \mu\text{mol}$
430 $\text{photons m}^{-2} \text{s}^{-1}$) allowing them to reach photosynthetic saturation. Therefore, at least during

431 the afternoon, when irradiances are maximal, fleshy epiphytic macroalgae may here protect
432 *L. corallioides* from photoinhibition and from any potential photodamage. Interactions with
433 other biotic and abiotic parameters may diminish or enhance these predicted effects. For
434 instance, reduced turbidity due to water renewal from tides and bottom currents or a reduction
435 in fleshy epiphytic macroalgae due to herbivorous grazing can maintain a favorable physico-
436 chemical environment for maerl under low irradiances. Nevertheless, our study highlights
437 the ambivalent relationship between maerl and its fleshy epiphytic macroalgae inhabiting
438 highly turbid and shallow temperate ecosystems such as the Bay of Brest.

439

440 *4.3 Heterogeneity of primary production in the Bay of Brest*

441 The comparison of macroalgal primary production (NPP) between the two maerl beds studied
442 here demonstrated that maerl bed primary production has heterogeneous spatio-temporal
443 patterns. In the Bay of Brest, variability in depth among stations translated into higher bottom
444 irradiances at Station B, and therefore higher algal NPP for both *L. corallioides* and its fleshy
445 epiphytic macroalgae. In this context, due to the lower irradiance required by algae to reach
446 photosynthetic saturation at Station B (i.e. E_k of $100 \mu\text{mol photon m}^{-2} \text{ s}^{-1}$ for both *L.*
447 *corallioides* and *S. chordalis*), maximal productivity can be reached, at least around noon,
448 but also during the morning and afternoon, depending on tidal height. However, at Station
449 A, maximal macroalgal productivity may only be reached when low tide occurs around noon
450 during high water spring tides. Due to the higher spatial heterogeneity of living *L.*
451 *corallioides* biomass in the maerl bed at Station A (1 to 9 kg DW m^{-2}) than at Station B (3–
452 6 kg m^{-2}) (Qui-Minet et al. 2018), maerl NPP showed higher variability at this location. The
453 contribution of fleshy epiphytic macroalgae to the NPP also varies with bottom irradiance.

454 Filamentous Rhodomelaceae have a significantly higher GPP_{MAX} than *S. chordalis*, but their
455 productivity is limited by incident light. When bottom light intensity is below $50 \mu\text{mol}$
456 $\text{photons m}^{-2} \text{s}^{-1}$, filamentous Rhodomelaceae and *S. chordalis* have similar NPP per m^2 . On
457 the other hand, above $400 \mu\text{mol photons m}^{-2} \text{s}^{-1}$, filamentous Rhodomelaceae can exceed the
458 value of *S. chordalis* NPP by two-fold. Nevertheless, according to our estimations for
459 summer 2015, maximal bottom irradiance at Station A was $300 \mu\text{mol photons m}^{-2} \text{s}^{-1}$ (around
460 noon and under a HWST) and thus, *L. corallioides* and its fleshy epiphytic macroalgal NPP
461 values were higher at Station B.

462 The impact of fleshy epiphytic macroalgae on maerl bed primary production depends on their
463 biomass and taxon composition, fleshy epiphytic algal biomass being similar between *S.*
464 *chordalis* (Station B) and filamentous Rhodomelaceae (Station A) (Qui Minet et al. 2018).
465 The differences in NPP between these epiphytic algae were mainly correlated with bottom
466 irradiance and their physiological rates. Despite significantly higher biomass of *L.*
467 *corallioides* relative to epiphyte biomass on maerl beds (fleshy epiphytic biomass was less
468 than 50 g DW m^{-2} at both stations, whereas maerl biomasses ranged from 0.85 to 8.5 kg DW
469 m^{-2} at Station A and from 3.1 to 5.6 kg m^{-2} at Station B, Qui-Minet et al. 2018), fleshy
470 epiphytic macroalgae had higher photosynthetic rates, and accounted for one fourth of maerl
471 bed NPP ($22 \pm 13\%$ and $24 \pm 0.02\%$ of NPP at stations A and B, respectively), independently
472 of tidal height and incident surface irradiance. Species interactions were not considered here,
473 but may affect these macroalgal productivity estimations. The relative contribution of *L.*
474 *corallioides* to the estimated NPP can be effectively overestimated due fleshy epiphytic
475 macroalgae shading the host *L. corallioides*. Consequently, fleshy epiphytic macroalgae may
476 actually have a relatively higher contribution to maerl bed productivity than estimated here.
477 Nevertheless, the shading effect of fleshy epiphytic macroalgae may also protect *L.*

478 *corallioides* from photo-inhibition under high irradiances, as occurs at Station B when
479 bottom irradiance is greater than the irradiance of photosynthetic saturation of *L. corallioides*
480 and *S. chordalis* ($> 100 \mu\text{mol photons m}^{-2} \text{s}^{-1}$) at Station B.

481 Due to the highly variable irradiance and tidal rhythms, significant daily changes in
482 macroalgal diel (24 h) NPP can be observed at each station through the summer season. When
483 the tide is high, summer days with low light intensity can lead to a negative macroalgal NPP
484 ($R > \text{GPP}$). This situation is more accentuated at the deepest station (Station A) and correlated
485 with the lower bottom irradiances at this location, which rarely reach saturating irradiances
486 for *L. corallioides* and filamentous Rhodomelaceae. Previous studies have defined maerl
487 beds in the Bay of Brest as heterotrophic communities, and maximal community respiration
488 measured during summer has been estimated at $2 \text{ g C m}^{-2} \text{ day}^{-1}$ (Martin et al. 2007), including
489 fleshy epiphytic macroalgae, the epiphytic microbiome (bacteria and microflora), the benthic
490 fauna and the microphytobenthos associated with the sediment (Martin et al. 2007). Although
491 this value may vary among maerl beds, according to our data, macroalgal (maerl and
492 epiphytes) contributions to the maerl bed community respiration are 29–31% at Station A
493 (21–24% for *L. corallioides* and 7% for filamentous Rhodomelaceae) and 22% at Station B
494 (17% for *L. corallioides* and 5% for *S. chordalis*). On the other hand, mean community GPP
495 in the Bay of Brest in summer has been estimated to be $1.3 \text{ g C m}^{-2} \text{ day}^{-1}$ (Martin et al. 2007).
496 According to our estimations, summer algal GPP represents 21% (Station A) and 35%
497 (Station B) of this value during low irradiance days, but would exceed this value by 15%
498 during high irradiance days ($1.5 \text{ g C m}^{-2} \text{ day}^{-1}$ at both stations A and B).

499

500 **5. CONCLUSIONS**

501 The impact of fleshy epiphytic macroalgae on maerl physiology is equivocal and it depends
502 on bottom incident irradiance, and therefore on the location of maerl beds and their specific
503 water depths and turbidity. Under low irradiances, fleshy epiphytic macroalgae will compete
504 with maerl for light, and under high irradiances they will protect maerl. The overall impact
505 of fleshy epiphytic macroalgae on maerl physiology not only depends on their abundance,
506 but on taxon composition and morphology (i.e. shading effect). In addition to the interaction
507 between coralline algae and their epiphytes, future research should also address other biotic
508 interactions such as grazing or interactions with local abiotic conditions, such as
509 hydrodynamic regimes, because they may preserve maerl algae from any potential negative
510 impact of their epiphytes.

511 At the ecosystem scale, bottom incident irradiance in coastal ecosystems is affected by
512 anthropogenic activities, including nutrients and organic matter, that may increase the
513 seawater turbidity and sedimentation rates. Our results highlight the importance of
514 monitoring the incident irradiance received by macroalgal species acting as ecosystems
515 engineers, because they play fundamental roles in biodiversity preservation and
516 biogeochemical cycles. Assessing maerl bed health and applying ecosystem management
517 policies to define threshold values of physico-chemical parameters (incident irradiance,
518 turbidity, nutrients release, etc.) thus requires better knowledge on the physiology of maerl
519 algae as well as of their fleshy epiphytes.

520 This is the first study to compare the physiological parameters of *Lithothamnion corallioides*
521 and its fleshy macroalgal epiphytes. This is also the first assessment of the contribution (~
522 25%) of fleshy epiphytic macroalgae to maerl bed C budgets. Although physiological rates
523 of maerl are significantly lower than those of fleshy epiphytic macroalgae, due to their high
524 living biomass in the Bay of Brest, their contribution to the C cycles is very high (~ 75% of

525 the total NPP). A more accurate estimation of the fleshy epiphytic macroalgae contribution
526 to maerl bed productivity requires studying their physiology under different environmental
527 conditions, such as temperature, irradiance or nutrient concentrations, throughout their period
528 of occurrence. Finally, this study is also among the first to assess the contribution of fleshy
529 epiphytic macroalgae to the primary production of coastal ecosystems dominated by
530 foundation macroalgal species.

531

532

533 **ACKNOWLEDGEMENTS**

534 We thank the crew of the R/V *Albert Lucas*, and in particular Franck and Daniel, for their
535 invaluable help with sampling. This work benefited from a grant from the Consejo Nacional
536 de Ciencia y Tecnología (CONACyT) and from support from French National Research
537 through the investment expenditure program IDEALG ANR-10-BTBR.

538

539 **REFERENCES**

- 540 Amado-Filho GM, Moura RL, Bastos AC, Salgado LT, Sumida PY, Guth AZ, Francini-Filho
541 RB (2012) Rhodolith beds are major CaCO₃ bio-factories in the tropical South West Atlantic.
542 PloS One 7:e35171
- 543
- 544 Amado-Filho GM, Bahia RG, Pereira-Filho GH, Longo LL (2017) South Atlantic Rhodolith
545 Beds: Latitudinal Distribution, Species Composition, Structure and Ecosystem Functions,
546 Threats and Conservation Status, in: Riosmena-Rodríguez R, Nelson W, Aguirre J (Eds.),
547 Rhodolith/Maërl Beds: A Global Perspective, Springer International Publishing, Cham,; pp.
548 299–317
- 549
- 550 Arar EJ, Collins GB (1997) Method 445.0: In Vitro Determination of Chlorophyll *a* and
551 Pheophytin *a* in Marine and Freshwater Algae by Fluorescence, Revision 1.2. ed. United
552 States Environmental Protection Agency, Office of Research and Development, National
553 Exposure Research Laboratory, Cincinnati, OH
- 554
- 555 Baweja P, Kumar S, Sahoo D, Levine I (2016) Chapter 3 - Biology of Seaweeds, in:
556 Fleurence J, Levine Ira (Eds.) Seaweed in Health and Disease Prevention. Academic Press,
557 San Diego, pp. 41–106
- 558
- 559 Berlinghof J, Peiffer F, Marzocchi U, Munari M, Quero GM, Dennis L, Wild C, Cardini U
560 (2022) The role of epiphytes in seagrass productivity under ocean acidification. Sci Rep 12:
561 6249
- 562
- 563 Borowitzka MA, Lavery PS, van Keulen M (2006) Epiphytes of seagrasses. In: Larkum

564 AWD, Orth, R.J. and Duarte, C.M., (eds.) Seagrasses: Biology, Ecology and Conservation.
565 Springer, Dordrecht, The Netherlands, pp. 441–462
566

567 Brodie J, Williamson CJ, Smale DA, Kamenos NA, Mieszkowska N, Santos R, Cunliffe M,
568 Steinke M, Yesson C, Anderson KM, Asnaghi V, Brownlee C, Burdett HL, Burrows MT,
569 Collins S, Donohue PJC, Harvey B, Foggo A, Noisette F, Nunes J, Ragazzola F, Raven JA,
570 Schmidh DN, Suggett D, Teichberg M, Hall-Spencer JM (2014) The future of the NE
571 Atlantic benthic flora in a high CO₂ world. *Ecol Evol* 4: 2787–2789
572

573 Buesa RJ (1980) Photosynthetic Quotient of Marine Plants. *Photosynthetica* 14 (3): 337–342
574

575 Bunker FSD, Brodie JA, Maggs CA, Bunker AR (2017) Seaweeds of Britain and Ireland:
576 Second Edition, Seasearch 312 pp. Plymton St. Maurice, Plymouth
577

578 Carvalho MC, Eyre B (2011) Carbon stable isotope discrimination during respiration in three
579 seaweed species. *Mar Ecol Prog Ser* 437: 41–49
580

581 Chalker (1981) Simulating light-saturation curves for photosynthesis and calcification by
582 reef-building corals. *Mar Biol* 63 (2): 135–141
583

584 Cornwall CE, Hepburn CD, Pilditch CA, Hurd CL (2013) Concentration boundary layers
585 around complex assemblages of macroalgae: Implications for the effects of ocean
586 acidification understory coralline. *Limnol Oceanogr* 58 (1): 121–130
587

588 Dawes CJ, Orduña-Rojas J, Robledo D (1999) Response of the tropical seaweed *Gracilaria*
589 *cornea* to temperature, salinity and irradiance. *J Appl Phycol* 10: 419–425
590

591 Dudgeon SR, Kübler JE, Vadas RL, Davison IR (1995) Physiological responses to
592 environmental variation in intertidal red algae : does thallus morphology matter? *Mar Ecol*
593 *Progr Ser* 117:193-206
594

595 Egilsdottir H, Noisette F, Noël LM-LJ, Olafsson J, Martin S (2013) Effects of *p*CO₂ on
596 physiology and skeletal mineralogy in a tidal pool coralline alga *Corallina elongata*. *Mar*
597 *Biol* 160: 2103–2112
598

599 Gattuso JP, Magnan A, Billé R, Cheung WWL, Howes EL, Joos F, Allemand D, Bopp L,
600 Cooley SR, Eakin CM, Hoegh-Guldberg O, Kelly RP, Pörtner HO, Rogers AD, Baxter JM,
601 Laffoley D, Osborn D, Rankovic A, Rochette J, Sumalia UR, Treyer S, Turley C (2015)
602 Contrasting futures for ocean and society from different anthropogenic CO₂ emissions
603 scenarios. *Science* 349
604

605 Grall J (2002) Biodiversité spécifique et fonctionnelle du maerl: réponses à la variabilité de
606 l'environnement côtier. PhD thesis, Université de Bretagne Occidentale
607

608 Guillou M, Grall J, Connan S (2002) Can low sea urchin densities control macro-epiphytic
609 biomass in a north-east Atlantic maerl bed ecosystem (Bay of Brest, Brittany, France)? J
610 Mar Biol Assoc UK 82: 867–876

611
612 Guiry MD in Guiry MD & Guiry GM (9 March 2020) *AlgaeBase*. World-wide electronic
613 publication, National University of Ireland, Galway. <https://www.algaebase.org>; (accessed
614 5 Jan 2022)

615
616 Guy-Haim T, Silverman J, Wahl M, Aguirre J, Noisette F, Rilov G (2020) Epiphytes provide
617 micro-scale refuge from ocean acidification. Mar Environ Res 161
618

619 Heijden L, Kamenos NA (2015) Reviews and syntheses: Calculating the global contribution
620 of coralline algae to total carbon burial. Biogeosciences 12: 6429–6441
621

622 Hurd CL (2000) Review: Water motion, marine macroalgal physiology, and production. J
623 Phycol 36: 452–472
624

625 Hernandez-Kantun JJ, Hall-Spencer JM, Grall J, Adey W, Rindi F, Maggs CA, et al. (2017)
626 North Atlantic Rhodolith Beds. In: Riosmena-Rodríguez R, Nelson W, Aguirre J, editors.
627 Rhodolith/Maërl Beds: A Global Perspective Cham: Springer International Publishing. p.
628 265–79
629

630 Hurd C, Harrison P, Druehl L (1996) Effects of seawater flow velocity on inorganic
631 nitrogen uptake by morphologically distinct forms of *Macrocystis integrifolia* from
632 sheltered and exposed sites. Mar Biol 126: 205–214.
633

634 Johansson G, Snoeijis P (2002) Macroalgal photosynthetic responses to light in relation to
635 thallus morphology and depth zonation. Mar Ecol Progr Ser 244: 63–72
636

637 Kroeker KJ, Kordas RL, Crim RN, Singh GG (2010) Meta-analysis reveals negative yet
638 variable effects of ocean acidification on marine organisms. Ecol Lett 13:1419–34
639

640 McCoy SJ, Santillán-Sarmiento A, Brown MT, Widdicombe S, Wheeler GL (2020)
641 Photosynthetic Responses of Turf-forming Red Macroalgae to High CO₂ Conditions. J
642 Phycol 56: 85–96
643

644 Martin S, Castets M-D, Clavier J (2006) Primary production, respiration and calcification
645 of the temperate free-living coralline alga *Lithothamnion corallioides*. Aquat Bot 85:121–
646 128
647

648 Martin S, Clavier J, Chavaud L, Thouzeau G (2007) Community metabolism in temperate
649 maerl beds. I. Carbon and carbonate fluxes. Mar Ecol Progr Ser 335: 19–29
650

651 Martin S, Charnoz A, Gattuso J-P (2013) Photosynthesis, respiration and calcification in the

652 Mediterranean crustose coralline alga *Lithophyllum cabiochae* (Corallinales, Rhodophyta).
653 Eur J Phycol 48 (2): 163–172
654

655 Martin S, Hall-Spencer JM (2016) Effects of ocean warming and acidification on
656 rhodolith/maerl beds. Rhodolith/maerl beds: a global perspective (eds Riosmena- Rodríguez
657 R, Nelson W & Aguirre J. Springer International Publishing, Cham
658

659 McCoy SJ, Kamenos NA (2015) Coralline algae (Rhodophyta) in a changing world:
660 integrating ecological, physiological, and geochemical responses to global change. J Phycol
661 51: 6–24
662

663 Michler T, Aguilera J, Hanelt D, Bischof K, Wiencke C (2002) Long-term effects of
664 ultraviolet radiation on growth and photosynthetic performance of polar and cold-temperate
665 macroalgae. Mar Biol 140: 1117–1127
666

667 Moncreiff CA, Sullivan MJ (2001) Trophic importance of epiphytic algae in subtropical
668 seagrass beds: evidence of multiple stable isotope analyses. MEPS 215: 93–106
669

670 Nelson WA (2009) Calcified macroalgae - critical to coastal ecosystems and vulnerable to
671 change: a review. Mar Freshw Res 60: 787–801
672

673 Olafsson E (2016) Marine Macrophytes as Foundation Species (1st ed.). CRC Press, Boca
674 Raton
675

676 Pedersen MF, Nejrup LB, Pedersen TM, Fredriksen S (2014) Sub-canopy light conditions
677 only allow low annual net productivity of epiphytic algae on kelp *Laminaria hyperborea*.
678 MEPS 516: 163–176
679

680 Peña V, Barbara I (2010) Seasonal patterns in the maerl community: case study of shallow
681 subtidal European Atlantic beds. Eur J Phycol 45 (3): 327–342
682

683 Peña, V, Bárbara I, Grall J, Maggs CA, Hall-Spencer JM (2014) The diversity of seaweeds
684 on maerl in the NE Atlantic. Mar Biodivers 44: 533–551
685

686 Qui-Minet ZN, Delaunay C, Grall J, Six C, Cariou T; Bohner O, Legrand E, Davoult D,
687 Martin S. (2018) The Role of Local Environmental Changes on Maerl and Its Associated
688 Non-Calcareous Epiphytic Flora in the Bay of Brest. Estuar Coast Shelf Sci 208: 140–152
689

690 Qui-Minet ZN, Davoult D, Grall J, Delaunay C, Six C, Cariou T, Martin S (2021) Physiology
691 of maerl algae: Comparison of inter- and intraspecies variations. J Phycol 57(3): 831–848
692

693 Riosmena-Rodríguez R, Nelson W, Aguirre J eds (2017) Rhodolith/Maerl Beds: A Global
694 Perspective: Springer International Publishing, Cham
695

696 Roleda MY, Hurd CL (2019) Seaweed nutrient physiology: application of concepts to
697 aquaculture and bioremediation. Phycologia 58 (2019) 552–562
698

699 Semesi IS, Beer S, Bjork M (2009) Seagrass photosynthesis controls rates of calcification
700 and photosynthesis of calcareous macroalgae in a tropical seagrass meadow. *Mar Ecol Progr*
701 *Ser* 382: 41–47
702

703 Schoenrock KM, Bacquet M, Pearce M, Rea BR, Schofield JE, Lea J, Mair D, Kamenos N
704 (2018) Influences of salinity on the physiology and distribution of the Arctic coralline
705 algae, *Lithothamnion glaciale* (Corallinales, Rhodophyta). *J Phycol* 54: 690–702
706

707 Short J, Kendrick GA, Falter J, McCulloch MT (2014) Interactions between filamentous turf
708 algae and coralline algae are modified under ocean acidification. *J Exp Mar Biol Ecol* 456:
709 70–77

710 Short JA, Pedersen O, Kendrick GA (2015) Turf algal epiphytes metabolically induce local
711 pH increase, with implications for underlying coralline algae under ocean acidification.
712 *Estuar Coast Shelf Sci* 164: 463–470
713

714 Sordo L, Santos R, Barrote I, Freitas C, Silva J (2020). Seasonal Photosynthesis,
715 Respiration, and Calcification of a Temperate Maërl Bed in Southern Portugal, *Frontiers in*
716 *Mar Sci* 7: 136.

717

718 Talarico L, Maranzana G (2000) Light and Adaptive Responses in Red Macroalgae: An
719 Overview. *J Photochem Photobiol B* 56 (1): 1–11

720 [1]

721 Wallentinus I (1984) Comparisons of nutrient uptake rates for Baltic macroalgae with
722 different thallus morphologies. *Mar Biol* 80: 215–225
723
724

725 **TABLES.**

726
727 **Table 1.**

728 Summary of the mean (\pm S.D.) parameters of photosynthesis-irradiance (P-E) curves for
729 filamentous Rhodomelaceae and *Solieria chordalis* (n = 5) and of Kruskal-Wallis tests (H)
730 to compare physiological parameters among taxa. GPP_{MAX} and R are the maximal gross
731 primary production and respiration rates, respectively, Ek is the irradiance of saturation, Ec
732 is the irradiance of compensation, R is the respiration rate, alpha (α) is the photosynthetic
733 efficiency. Bold values indicate statistical significance at $p < 0.05$. *** $p < 0.001$; ** $p < 0.01$;
734 * $p < 0.05$.

Parameter	Filamentous Rhodomelaceae	<i>Solieria chordalis</i>	Comparison among species	
			H	p-value
GPP _{MAX} ($\mu\text{mol O}_2 \text{ g}^{-1} \text{ DW h}^{-1}$)	245 \pm 54	144 \pm 8	4.8	<0.05*
R ($\mu\text{mol O}_2 \text{ g}^{-1} \text{ DW h}^{-1}$)	24 \pm 2	15 \pm 3	6.8	<0.01**

Ek ($\mu\text{mol photons m}^{-2} \text{ s}^{-1}$)	185 \pm 90	115 \pm 26	6.6	<0.01**
Ec ($\mu\text{mol photons m}^{-2} \text{ s}^{-1}$)	19 \pm 4	12 \pm 3	11.5	<0.01**
α $\mu\text{mol O}_2 \text{ g}^{-1} \text{ DW h}^{-1} (\mu\text{mol photons m}^{-2} \text{ s}^{-1})^{-1}$	1.0 \pm 0.3	1.4 \pm 0.4	8.2	<0.05*
GPP _{MAX} ($\mu\text{mol O}_2 \text{ mg}^{-1} \text{ Chl } a \text{ h}^{-1}$)	114 \pm 58	206 \pm 11	12.5	<0.01**
α ($\mu\text{mol O}_2 \text{ mg}^{-1} \text{ Chl } a \text{ h}^{-1} (\mu\text{mol photons m}^{-2} \text{ s}^{-1})^{-1}$)	0.6 \pm 0.3	1.9 \pm 0.7	8.2	<0.05*

735

736

737

738

739

740

741

742

743

Table 2. Summary of Kruskal-Wallis tests used to compare the physiological parameters between non-calcareous epiphytic macroalgae and *Lithothamnion corallioides* at stations A and B (n = 5). GPP_{MAX} and R are the rates of maximal gross primary production and respiration, respectively, expressed per unit of Chl *a* ($\mu\text{mol O}_2 \text{ mg}^{-1} \text{ Chl } a \text{ h}^{-1}$), Ek is the irradiance of saturation ($\mu\text{mol photons m}^{-2} \text{ s}^{-1}$), Ec is the irradiance of compensation ($\mu\text{mol photon m}^{-2} \text{ s}^{-1}$), and α ($\mu\text{mol O}_2 \text{ mg}^{-1} \text{ Chl } a \text{ O}_2 \text{ mg}^{-1} \text{ Chl } a \text{ h}^{-1} (\mu\text{mol photons m}^{-2} \text{ s}^{-1})^{-1}$) is the photosynthetic efficiency. Bold values indicate statistical significance at $p < 0.05$. *** $p < 0.001$; ** $p < 0.01$; * $p < 0.05$

Parameters	Station A		Station B	
	H	p-value	H	p-value
NPP	6.82	0.009**	6.82	0.009**
R	6.82	0.009**	6.82	0.009**
Ek	0.27	0.602	0.53	0.465
Ec	0.53	0.465	0.53	0.465
α	6.82	0.009**	6.82	0.009**

744

745

746

747

Table 3. Summary of Kruskal Wallis tests used to compare estimated bottom irradiances between stations and within stations over the course of the summer season. Bold values indicate statistical significance at $p < 0.05$. *** $p < 0.001$; ** $p < 0.01$; * $p < 0.05$

Comparison of bottom irradiance ($\mu\text{mol photon m}^{-2} \text{ s}^{-1}$) between stations								
	Early morning		Late morning		Afternoon		Evening	
	H	p-value	H	p-value	H	p-value	H	p-value
Station A vs. B	6.4	0.001***	11.5	<0.001***	77.4	<0.001***	77.4	<0.001***
Comparison between days of bottom irradiance ($\mu\text{mol photon m}^{-2} \text{ s}^{-1}$)								
	Early morning		Late morning		Afternoon		Evening	

	H	p-value	H	p-value	H	p-value	H	p-value
Station A	71.5	<0.001***	144.1	<0.001***	229.5	<0.001***	80.1	<0.001***
Station B	80.8	<0.001***	167.4	<0.001***	222.4	<0.001***	66.7	<0.001***

748

749 **Table 4.** Summary of Kruskal-Wallis tests used to compare the rates of net primary
750 production (in mg C m⁻² h⁻¹) per m⁻² h⁻¹ in filamentous Rhodomelaceae (Station A), *S.*
751 *chordalis* (Station B) and *L. corallioides* (stations A and B) under high water spring tide
752 (HWST), mean water tide (MWT) and low water neap tide (LWNT), during the early
753 morning, late morning, afternoon and evening (n> 10). Bold values indicate statistical
754 significance at p < 0.05. *** p < 0.001; ** p < 0.01; * p < 0.05.

	C (mg m ⁻² h ⁻¹)							
	Early morning		Late morning		Afternoon		Evening	
	H	p-value	H	p-value	F	p-value	F	p-value
Filamentous Rhodomelaceae Tides	11.3	<0.01**	15.8	<0.001***	22.5	<0.001***	19.3	<0.001***
	HWST > LWNT MWT = LWNT		HWST < MWT & LWNT		HWST & MWT > LWNT		LWNT & MWT > HWST	
<i>S. chordalis</i> : Tides	8.8	<0.05*	11.5	<0.01**	28.2	<0.001***	17.1	<0.001***
	Inconclusive		Inconclusive		HWST > MWT > LWNT		LWNT & MWT > HWST	
<i>L. corallioides</i> Station A: Tides	11.3	<0.01**	15.8	<0.001***	22.5	<0.001***	19.3	<0.001***
	HWST > LWNT, HWST > MWT MC = LC		HWST > MWT, HWST > LWNT, HWST = MWT		HWST & MWT > LWNT		MWT & LWNT > HWST	
<i>L. corallioides</i> Station B: Tides	12.4	<0.01**	17.1	<0.001***	23.2	<0.001***	19.7	<0.001***
	HWST = MWT LWNT & MWT > HWST		LWNT > HWST & MWT		HWST & MWT > LWNT		LWNT & MWT > HWST	

755

756

757

758

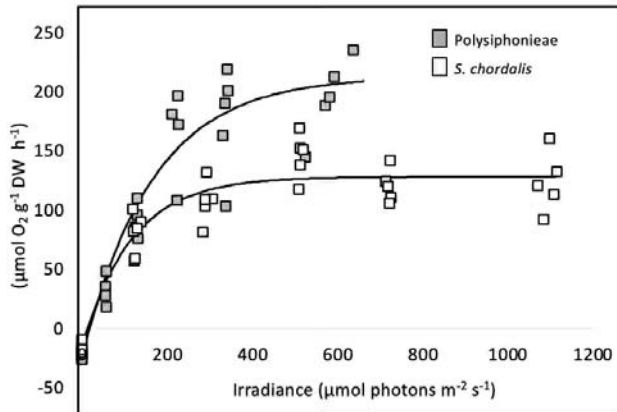
759

760

761

762 FIGURES

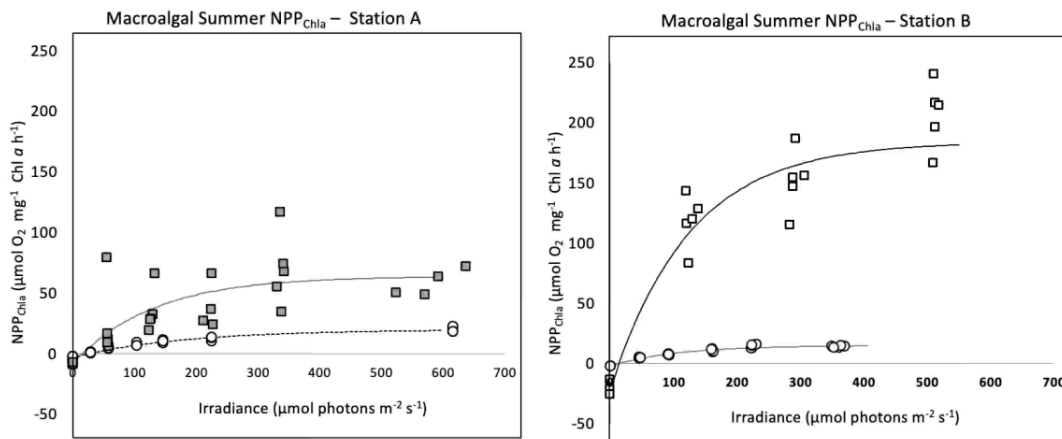
763



764

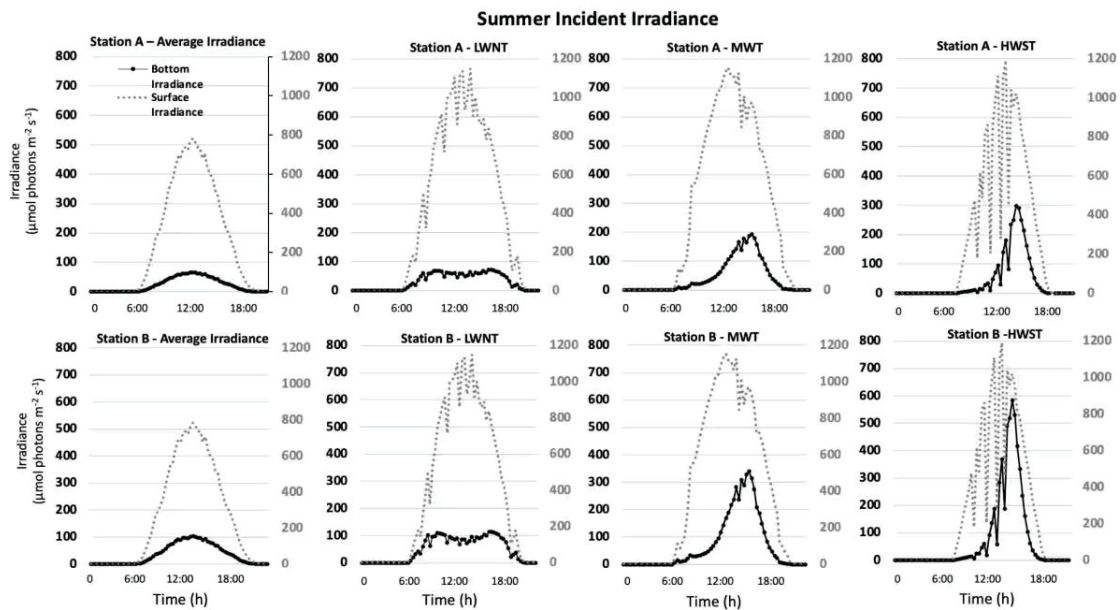
765 **Figure 1.** Relationship between net primary production (in O₂ flux per algal g DW) and
 766 irradiance ($\mu\text{mol photons m}^{-2} \text{s}^{-1}$) in summer in filamentous Rhodomelaceae (dark squares)
 767 and *Solieria chordalis* (white squares).

768



769

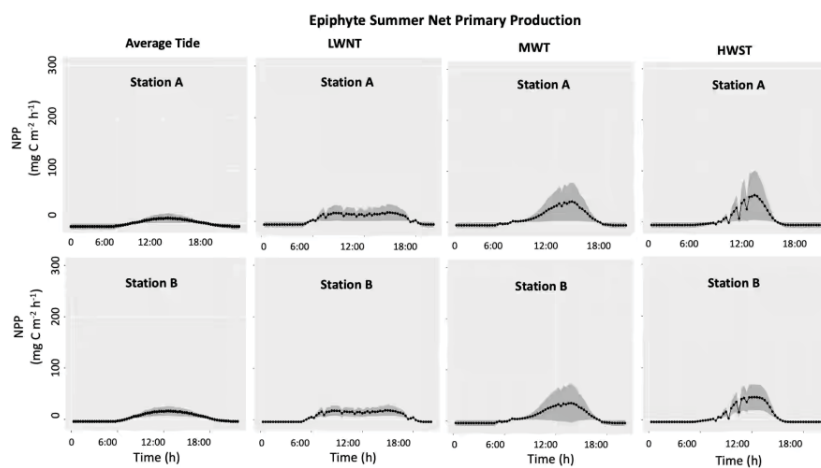
770 **Figure 2.** Relationship between net primary production per Chl *a* content (in O₂ flux per mg
 771 Chl *a*) and irradiance ($\mu\text{mol photons m}^{-2} \text{s}^{-1}$) in summer in *Lithothamnion corallioides* (white
 772 dots), and filamentous Rhodomelaceae at Station A (gray squares) and *L. corallioides* (white
 773 dots) and *Solieria chordalis* (white squares) at Station B.



774

775 **Figure 3.** Estimated 24-h bottom irradiance at Station A and Station B considering average
 776 summer bottom incident irradiance and during specific summer days with low water neap
 777 tide (LWNT, 1 September 2015), medium water tide (MWT, 20 June 2015), and high water
 778 spring tide (HWSP, 25 June 2015).

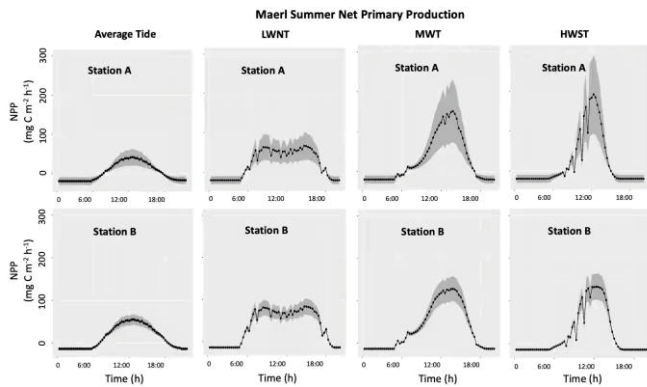
779



780

781 **Figure 4.** Estimated mean net primary production over 24 h in filamentous Rhodomelaceae
 782 at Station A and *Solieria chordalis* at Station B, from average summer bottom incident
 783 irradiance and during specific summer days with low water neap tide (LWNT, 1 September
 784 2015), medium water tide (MWT, 20 June 2015), and high water spring tide (HWSP, 25 June

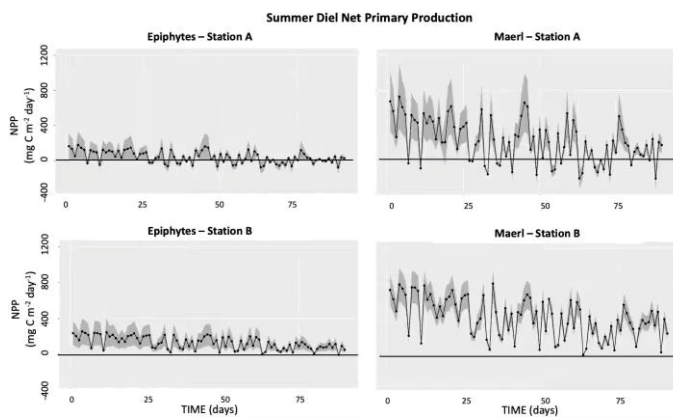
785 2015). The shaded area represents the standard deviation as a function of the heterogeneity
786 of *Lithothamnion corallioides* biomass at stations A and B, respectively (n = 5).
787



747

748 **Figure 5.** Estimated mean net primary production over 24 h considering average bottom
 749 irradiance during summer season in *Lithothamnion corallioides* at stations A and B, from
 750 average summer bottom incident irradiance and during specific summer days with low
 751 water neap tide (LWNT, 1 September 2015), medium water tide (MWT, 20 June 2015),
 752 and high water spring tide (HWSP, 25 June 2015). The shaded area represents the
 753 standard deviation as a function of the heterogeneity of *L. corallioides* biomass at stations
 754 A and B, respectively (n = 5).

755



756

757 **Figure 6.** Estimated diel (24-h) net primary production in epiphytes (filamentous
 758 Rhodomelaceae and *Solieria chordalis*) and *Lithothamnion corallioides* at stations A and
 759 B during the summer season. The shaded area represents the standard deviation as a
 760 function of the heterogeneity of macroalgal biomass at stations A and B, respectively (n
 761 = 5).

762 APPENDICES/SUPPLEMENTARY FIGURES

763

764

765 **Figure 1.** Estimated daily bottom irradiance at station A during the summer season.

766

767

768 **Figure 2.** Estimated daily bottom irradiance at station B during the summer season.